PAPER

Infrared thermographic investigation on the ocular surface temperature of normal subjects

IOP Publishing *Physiol. Meas.* **41** (2020) 045003 (10pp) https://doi.org/10.1088/1361-6579/ab6b48

Physiological Measurement

IPEM Institute of Physics and Engineering in Medicine

PAPER

Infrared thermographic investigation on the ocular surface temperature of normal subjects

Sara Matteoli[1,4], **Federica Vannetti**[2,4], **Andrea Sodi**[3] **and Andrea Corvi**[1]

[1] Bioengineering laboratory, Department of Industrial Engineering, University of Florence, Florence, Italy
[2] IRCCS Fondazione don Carlo Gnocchi, Rehabilitation Center, Florence, Italy
[3] Department of Surgery and Translational Medicine, Eye Clinic, Careggi Teaching Hospital, University of Florence, Florence, Italy
[4] These authors contributed equally to this work.

E-mail: fvannetti@dongnocchi.it

RECEIVED
7 June 2019

REVISED
8 January 2020

ACCEPTED FOR PUBLICATION
14 January 2020

PUBLISHED
5 May 2020

Keywords: age-related ocular temperature, physiology of the eye, infrared image processing, thermographic acquisition

Abstract

Objective: It is understood that the ability to measure ocular temperature accurately will increase understanding of ocular physiology and should be a support in decision-making in classical diagnostic procedures. The use of ocular thermography offers great opportunities for monitoring the temperature of the anterior eye and analyzing the effects of certain pathologies on ocular surface temperature (OST). The aim of the present work is to measure the OST of 220 healthy normal subjects, stratified according to gender and age, in order to obtain a normal temperature distribution to be used as reference values when comparing healthy versus pathological conditions. *Approach*: The OST is measured from five regions, located over the whole area of the anterior eye, which correspond to particular anatomic structures, through a semi-automated procedure to post-process the infrared images. The relationship between OST and independent variables (forehead skin temperature, age, gender, level of physical activity, cardiovascular risk factors including sedentary lifestyle and smoking, laboratory temperature, and laboratory humidity) was investigated through linear regression models. *Main results*: The OSTs measured from the five different ocular regions are statistically different (p-value < 0.001), even when dividing our subjects into males and females, with the nasal cantus being the hottest region and the central cornea the coolest; when considering also the effect of age, stratifying our subjects into young, middle-aged and elderly, the OST decreases when age increases significantly. Statistical analysis based on linear regression models pointed out that age, forehead skin temperature, and lab temperature are the main factors to be taken into account when exploring the OST. *Significance*: As OST evaluation can be important in detecting different ocular pathologies, having precise details of the variation in temperature across the ocular surface and therefore a more detailed map of the OST adjusted according to subject characteristics and environment conditions could enhance early diagnosis and thus course of treatments.

1. Introduction

Interest in ocular temperature has spanned almost the last 100 years (Hardy 1934, Holmberg 1952, Fatt and Forester 1972), but accurate quantitative measurements of the ocular surface temperature (OST) have been possible only in the last few decades, thanks to non-invasive techniques such as infrared thermography (Mapstone 1968, Efron *et al* 1989, Morgan *et al* 1993, Ring and Ammer 2000, Purslow and Wolffsohn 2005, Tan *et al* 2009, Ring and Ammer 2012, Faust *et al* 2014). It is widely known that the ability to measure ocular temperature accurately will increase understanding of the ocular physiology and should be a decisional support to therapy integrated with classical diagnostic procedures. The use of ocular thermography offers great opportunities for monitoring the temperature of the anterior eye and analysing the effects of some pathologies on OST (Martin and Fatt 1986, Fujishima *et al* 1996, Cardona *et al* 1996, Mori *et al* 1997, Betney *et al* 1997, Morgan *et al* 1999, Craig *et al* 2000, Purslow *et al* 2005, Corvi *et al* 2006, Sodi *et al* 2007, Galassi *et al* 2007, Purslow and Wolffsohn

2007, Galassi *et al* 2008, Chang *et al* 2008, Sodi *et al* 2009,2014, Acharya *et al* 2009,2014,2015, Tan *et al* 2010a,2016, Kamao *et al* 2011, Su *et al* 2011, Vannetti *et al* 2014, Mencucci *et al* 2015, Matteoli *et al* 2016, 2017).

The literature offers only a few papers which analyse OST in normal subjects (Efron *et al* 1989, Morgan *et al* 1999, Purslow and Wolffsohn 2007, Acharya *et al* 2009, Tan *et al* 2009). From these papers some limitations can be recognised about the number of subjects tested, the age-range considered, the ocular area investigated, as well as the image post-processing procedure. Specifically, most of the papers consider only the temperature of the central ocular area or the average temperature of the whole ocular surface.

Furthermore, there is a large variability in the methods applied to post-processing measurements which influences the final results: some studies use manual procedures to identify the region the OST is calculated from (Efron *et al* 1989, Morgan *et al* 1995,1999, Fujishima *et al* 1996, Cardona *et al* 1996, Mori *et al* 1997, Murphy *et al* 1999, Craig *et al* 2000, Purslow *et al* 2005, Chiang *et al* 2006, Sodi *et al* 2007,2009,2014, Galassi *et al* 2007,2008, Purslow and Wolffsohn 2007, Chang *et al* 2008, Kamao *et al* 2011, Su *et al* 2011, Vannetti *et al* 2014); others use semi-automated techniques to segment an ocular region of interest (Acharya *et al* 2009, Tan *et al* 2010b, Matteoli *et al* 2018).

The aim of the present work is to measure the OSTs belonging to a sample of 220 healthy normal subjects, stratified according to gender and age, in order to obtain a normal temperature distribution to be used as referee values when comparing healthy versus pathological conditions. Specifically, the OST is measured from five regions, located on the whole area of the anterior eye, which correspond to particular ocular anatomic structures. Indeed, the temperature of these different regions can show different patterns depending on the particular ocular pathology (e.g. dry eye, age-related macular degeneration, uveal lesions, etc). For this reason, it is extremely important not to limit the OST analysis to the central part of the anterior eye.

2. Materials and methods

2.1. Participants

Two hundred and twenty subjects were enrolled in this study. Table 1 shows the demographic and anthropometric characteristics of the subjects, grouped according to sex and age.

The study complied with the Declaration of Helsinki and was approved by the Institutional Review Board at the University of Florence. Informed consent was obtained from each patient after explanation of the purpose and description of the procedures of the study. The presence of ocular or systemic pathologies was carefully investigated. Specifically, the exclusion criteria were as follows: glaucomatous optic neuropathy, high myopia, retinal angiomatous proliferation, polypoidal choroidal vasculopathy and other retinal and choroidal diseases, corneal or tear film abnormalities, diabetes mellitus and a body temperature higher than 37.5 °C. For each subject anamnestic information was collected, focusing on the presence of cardiovascular risk factors and smoking history, because some ocular pathologies are related to the presence of these conditions.

2.2. Experimental protocol

Thermographic acquisitions were performed for each subject by following the same protocol. The subject remained in the test room for 20 min, so that body temperature could adapt to the climatic condition of the room (Morgan 1994). Then, the subject's chin was positioned on an ophthalmic chinrest in front of a thermal camera, the lens of which (25 degrees built in) was positioned 300 mm from the subject's eyes, so that both eyes could be visualized in the same thermograms. Subjects were asked (i) to keep both eyes closed for 10 s before starting the measurement, so that the tear film was at its initial condition; (ii) to keep both eyes wide open, without any blinking, during the thermographic acquisition (7 s at 30 Hz). Subjects were instructed not to use beforehand any ocular lubricants, and not to smoke or drink hot beverages for at least 2 h before the thermographic examination, which was performed between 9:00 am and noon.

The thermal camera used was a FLIR 320A (FLIR Systems, Oregon, USA) with a focal plane sensor array size of 320 × 240 pixels and image frequency of 30 Hz. The detector's time constant was 12 ms with a measurement traceability of ±2% of reading and a noise equivalent temperature difference (NETD) of 0.07 °C at +30 °C, with emissivity set to 0.98. OST measurements were performed in a controlled room environment, illuminated with neon lights at the 'Maria Bouturlin' health centre in Barberino di Mugello, Florence, Italy. Both temperature and humidity were constantly monitored and maintained at an average of 24.6 °C ± 2.1 °C and 56% ± 8%, respectively.

For each thermographic acquisition only the first frame corresponding to the eye opening was selected for further analysis, in order to avoid the influence of tear-film evaporation (Morgan 1994). A typical thermographic image is shown in figure 1.

Forehead skin temperature was measured using an infrared thermometer applied on the forehead (RY210, Santamedical, USA) before starting the thermographic acquisition.

Table 1. Characteristics of the enrolled population.

	Age group[a]				
	Young	Middle-age	Elderly	Total	*p*-value[b]
Number of subjects	94	83	43	220	—
Female	47	42	19	108	—
Male	47	41	24	112	—
Age [years]					
Female	27.7 ± 6.7	50.9 ± 6.2	71.4 ± 5.6	44.4 ± 17.6	—
Male	25.3 ± 5.3	53.2 ± 6.9	72.9 ± 6.6	45.7 ± 19.9	—
p-value[c]	0.0670	0.1048	0.4376	0.5913	
Body mass [kg]					
Female	62.2 ± 12.8	65.0 ± 10.6	67.3 ± 13.7	64.2 ± 12.2	0.2166
Male	75.5 ± 10.8	79.9 ± 11.3	81.2 ± 10.4	78.3 ± 11.1	0.0615
p-value[c]	0.0000	0.0000	0.0005	0.0000	
Height [m]					
Female	1.65 ± 0.05	1.63 ± 0.06	1.63 ± 0.05	1.64 ± 0.06	0.142
Male	1.78 ± 0.07	1.75 ± 0.08	1.71 ± 0.08	1.75 ± 0.08	*0.0006*
p-value[c]	0.0000	0.0000	0.0002	0.0000	
Skin temperature [°C]					
Female	36.3 ± 0.4	36.1 ± 0.4	36.0 ± 0.4	36.2 ± 0.4	*0.0196*
Male	36.2 ± 0.4	36.1 ± 0.4	36.1 ± 0.5	36.1 ± 0.4	0.0535
p-value[c]	0.4209	0.5508	0.5565	0.5100	
Sedentary [Yes/No]					
Female	1/46	5/37	4/15	10/98	*0.042*
Male	2/45	3/38	2/22	7/105	0.750
p-value[c]	0.557	0.479	0.232	0.403	
Smoke [Yes/No]					
Female	15/32	13/29	5/14	33/75	0.903
Male	22/25	19/22	5/19	46/66	0.075
p-value[c]	0.195	0.250	0.365	0.207	
Cardiovascular risk [Yes/No]					
Female	1/46	9/33	12/7	22/86	<0.0001
Male	2/45	9/32	18/6	29/83	<0.0001
p-value[c]	0.557	0.954	0.401	0.332	

[a] Young = 18–40 years; middle-age = 41–64 years; elderly = over 65 years.
[b] The *p*-value shows whether there are significant differences between age groups for each characteristic.
[c] The *p*-value shows whether there are significant differences between males and females for each characteristic.

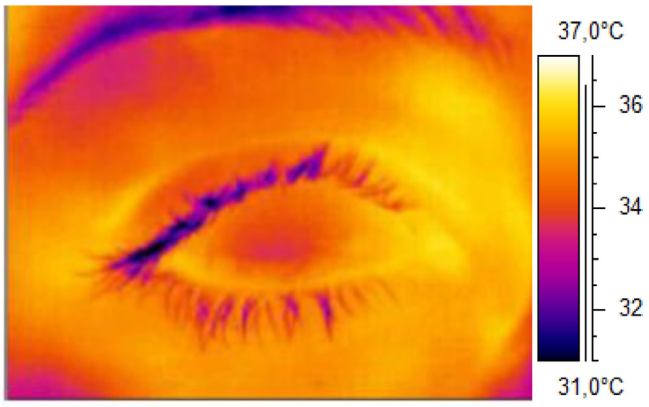

Figure 1. Typical thermographic image of the anterior eye.

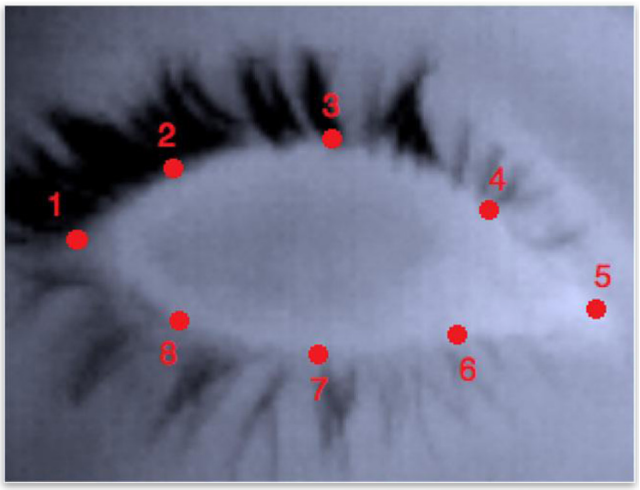

Figure 2. The eight points placed on the outline of the eye by the operator in order apply the semi-automatic procedure for the OST normalization.

2.3. Image processing

The image processing procedure was developed in Matlab (R2014, Mathworks, USA) (Matteoli *et al* 2018). This imaging procedure allows the processing of thermographic images, measuring the OST and visualizing the ocular thermal maps in a fast, reliable and reproducible way (Matteoli *et al* 2018). The strength of this new method is that the measured OSTs do not depend on the ocular geometry, hence it is possible to compare ocular profiles belonging to the same subject (right and left eye) as well as to different populations (Matteoli *et al* 2018).

In order to apply the ocular normalization, the operator has only to select eight points placed on the outline of the eye (figure 2). From the normalized images it is then possible to extrapolate automatically the OST from 31 points distributed on the ocular surface, each one covering a 3×3 pixel matrix. These points are obtained as an intersection between a series of parallel vertical lines and a horizontal line passing through the middle of the image and two curves reproducing 1/3 and 2/3 scaled versions of the normalizing model. Points located in the two canti are not evaluated as single points, but they represent the average temperature of both canti's area.

Figure 3 shows the eye divided into five main ocular areas corresponding to different anatomic structures: temporal cantus (1), temporal-central region (2), central cornea (3), central-nasal region (4), nasal cantus (5). The temperature of each area is calculated as the average of the points that compose it.

The image processing procedure was applied to only one frame, corresponding to the lids opening, of the entire thermographic sequence acquired in order to avoid the influence of the tear-film evaporation on OST.

2.4. Statistical analysis

Statistical analyses were carried out by means of STATA software (version SE 13.0, Texas, USA). A Student's *t*-test was used to compare OSTs belonging to the right and left eyes. An Anova test for repeated measures with Bonferroni correction was used to compare the OST measured from the five ocular regions according to sex stratified by age groups. A Shapiro–Wilk's W test was used to verify the normality of the data, and the effect size was estimated using a Cohen coefficient.

A multivariable linear regression allowed us to investigate the effect of independent variables, such as age, sex, skin temperature, lab temperature, lab humidity, smoking history, level of physical activity, and the presence of cardiovascular risk factor/pathologies on the OST, measured from the five ocular regions. A backward variables selection was applied in order to attain a more defined model, with a significance level of 0.05.

A p-value of < 0.05 was chosen to indicate a significant statistical difference.

3. Results

Among the 220 enrolled subjects, 152 subjects had a vision impairment due to refractive errors, which were corrected by daily use of glasses or contact lenses; thus, they were not excluded from the study. Furthermore, among the 220 enrolled subjects, 79 subjects were smokers or ex-smokers for less than 15 years, 69 subjects reported an absent or very low level of physical activity and 51 subjects had a cardiovascular pathology treated with drugs or were exposed to cardiovascular risk factors (presence of hypertension and/or dyslipidaemia). Table 1 describes the enrolled population, grouped by age and sex.

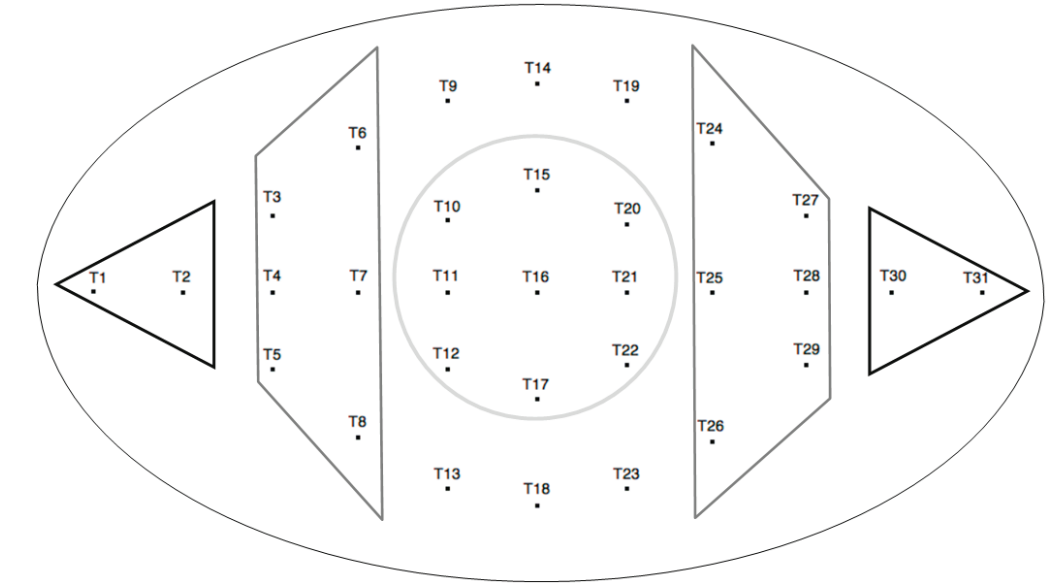

Figure 3. The 31 points distributed on the ocular surface are grouped into seven main areas. Starting from the left: (1) temporal cantus, (2) temporal-central region, (3) central cornea, (4) central-nasal region, (5) nasal cantus.

The comparison between OST belonging to right and left eye performed through a Student's *t*-test did not show a significant difference (p-value $= 0.62$, difference standard error $= 0.013$). So, our statistical analysis took into consideration data belonging to the right eye.

Figure 4 shows the average OST values $\pm$ standard deviation of the five ocular regions considered according to sex.

The normal distribution of the data was verified by using a Shapiro–Wilk's W test; the probability value range is between 0.274 and 0.993. We also tested the effect size by Cohen coefficient, which was higher than 0.8 in all comparisons with a p-value lower than 0.05.

The Anova test for repeated measures with Bonferroni correction showed a significant statistical difference among the five regions; specifically, paired comparisons gave a p-value <0.0001 both for male and female groups, except when comparing the OST of the central cornea against the temporal-central region within females (p-value $= 1.000$). Statistical comparison between male and female OSTs, carried out for each ocular region, did not show any significant difference (p-value >0.093).

Furthermore, figure 5 shows the average OST values $\pm$ standard deviation of the five ocular regions considered, with subjects divided into males and females, and stratified by age groups. Results obtained by Anova test for repeated measures with Bonferroni correction showed a different behaviour between males and females: within males the OSTs of young subjects was always significantly different compared to the OST of the other age-groups (p-value < 0.0001), whereas middle age and elderly subjects had similar OST values (p-value $= 1.000$); within females there was instead a significant difference among the OSTs of all three age-groups (p-value < 0.0001).

Table 2 shows the regression models applied for each ocular region. The statistical results highlight that the OST nasal regions are significantly correlated to subject factors (age and body/skin temperature), while cornea and temporal regions are significantly correlated to the same subject factors and also environmental conditions (laboratory temperature).

4. Discussion

The aim of the present work was to measure the OSTs belonging to a sample of 220 healthy normal subjects, considering differences due to sex and age, in order to obtain a normal temperature distribution. Such findings could be clinically useful when used as reference values comparing healthy versus pathological conditions. Specifically, the OST is measured from five regions, located on the whole area of the anterior eye, which correspond to particular ocular anatomic structure (temporal cantus, temporal-central region, central cornea, central-nasal region, nasal cantus).

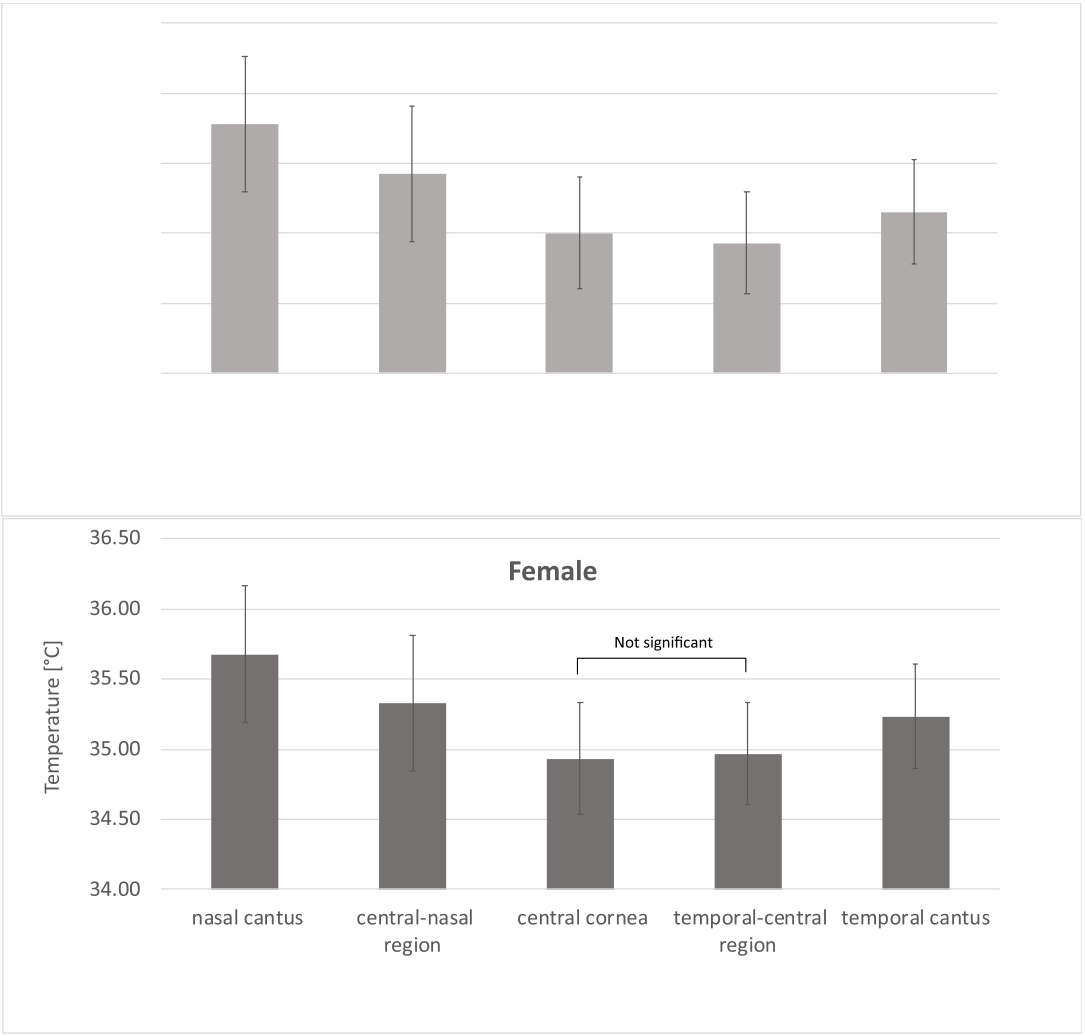

Male	35.78 ± 0.49	35.42 ± 0.49	35.00 ± 0.48	34.93 ± 0.45	35.15 ± 0.44
Female	35.68 ± 0.49	35.33 ± 0.48	34.93 ± 0.46	34.97 ± 0.48	35.23 ± 0.48

Figure 4. Mean OST values of the five ocular areas grouped by gender. All comparisons were statistically significant ($p < 0.0001$) except central cornea versus temporal-central region within female group (p-value $= 1.000$).

As reported by Purslow *et al* (2005) and Acharya *et al* (2009), the comparison between the OST distribution of right and left eyes did not show any significant statistical difference; hence the data analysis was carried out considering only the values related to the right side of all subjects.

Results shown in figure 4 indicate that OSTs measured from the five different ocular regions are statistically different (p-value < 0.001), even when dividing our subjects into males and females, with nasal cantus being the hottest region and the central cornea the coolest. This temperature distribution is mainly due to the blood perfusion. Indeed, the nasal cantus is the area nearest to the nasal arteria, so its temperature reflects the blood temperature running through that vessel; on the contrary, the central cornea shows the coolest temperature because it is anatomically avascularised and its temperature mainly depends on the tear film distribution as well as the environmental conditions (Efron *et al* 1989, Morgan *et al* 1993, Tan *et al* 2009).

When making a comparison between males and females based on the OST distribution of the five regions, without considering the age effect on the temperature, no differences were found (p-value > 0.093) (Efron *et al* 1989, Tan *et al* 2009). Instead, when considering also the effect of age, stratifying our subjects into young, middle-aged and elderly, the OST decreases when age increases (Morgan 1994, Morgan *et al* 1999) and some significant differences between males and females come to light. Specifically, within males the young group compared to the others always exhibited the hottest and most significant temperature difference in all regions ($p < 0.0001$), while there is no difference between middle-aged and elderly groups (p-value $= 1.000$). Within females, the OST shows a progressive significant decrease, so that all three age groups are statistically different. This age-related behaviour may be explained by considering the aging sex-dependent factors, e.g. the different hormonal profiles through life, associated with changes in the physiological functioning of the endocrine system (Morgan 1994).

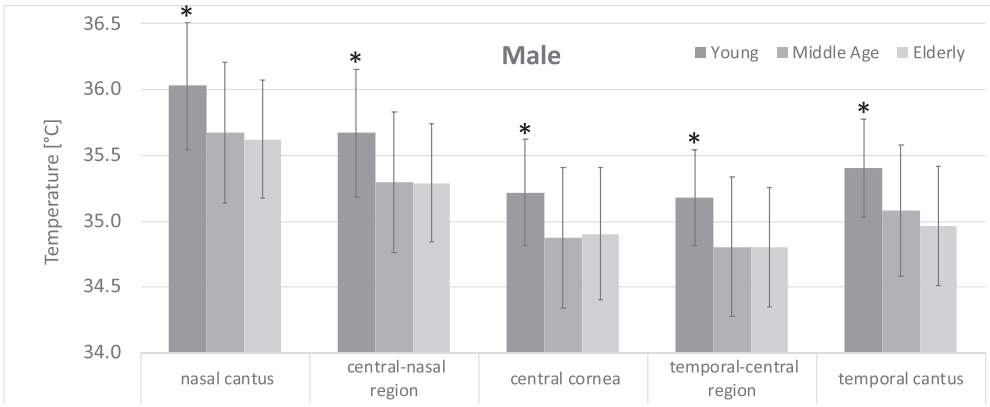

Male	Nasal cantus	Central-nasal region	Central cornea	Temporal-central region	Temporal cantus
Young	36.03 ± 0.48	35.67 ± 0.48	35.22 ± 0.40	35.18 ± 0.36	35.41 ± 0.37
Middle Age	35.68 ± 0.53	35.30 ± 0.53	34.88 ± 0.53	34.81 ± 0.53	35.09 ± 0.50
Elderly	35.62 ± 0.45	35.29 ± 0.45	34.91 ± 0.50	34.8 ± 0.45	34.96 ± 0.46

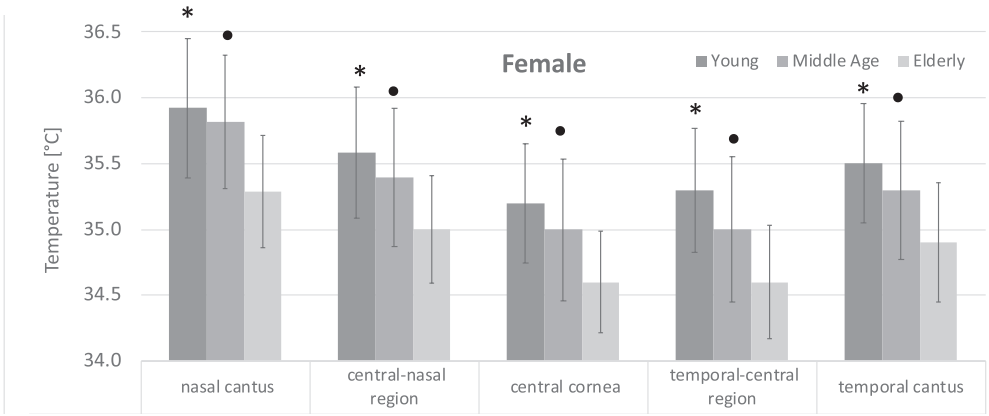

Female	Nasal cantus	Central-nasal region	Central cornea	Temporal-central region	Temporal cantus
Young	35.92 ± 0.53	35.59 ± 0.50	35.20 ± 0.45	35.30 ± 0.47	35.50 ± 0.45
Middle Age	35.82 ± 0.50	35.40 ± 0.53	35.00 ± 0.54	35.00 ± 0.55	35.30 ± 0.52
Elderly	35.29 ± 0.43	35.00 ± 0.41	34.60 ± 0.39	34.60 ± 0.43	34.90 ± 0.45

* = The OST of Young subjects is significantly different from Middle-age and Elderly subjects

• = The OST of Middle-age subjects is significantly different from Elderly subjects

Figure 5. Mean OST values of the five ocular areas grouped by age and gender.

Having a sample ranging over a large span of ages for both male and female subjects allows exploration of the OST distribution in a more accurate way, taking into consideration physiological differences.

In order to investigate the main subject-related factors (age, sex, body/forehead skin temperature, smoking history, level of physical activity, and the presence of cardiovascular risk factor/pathologies) as well as the environmental conditions (laboratory temperature and humidity) which may affect the OST, this study suggests a multi-variable linear regression. Statistical results pointed out that the OST nasal regions are significantly correlated to subject factors (age and body/forehead skin temperature), while cornea and temporal regions are significantly correlated to the same subject factors and also environmental conditions (laboratory temperature). Specifically, forehead skin temperature and laboratory temperature always have a positive coefficient, whereas an age increase is associated with a decrease of OST, with the same coefficient in all regression models, equal to −0.01 °C per year (see table 2). The negative effect of age on the OST might be related to the reduction of ocular blood supply with age and a variation of the tear film, which may result a slightly cooler OST than younger subjects (Morgan *et al* 1999).

This method could be a useful tool when evaluating the OST distribution; indeed, even though the literature points out that the abovementioned factors and conditions cannot be neglected (Efron *et al* 1989, Morgan *et al* 1993,1999, Morgan 1994, Tan *et al* 2009), there is a lack of a comprehensive model. Morgan *et al* (1993) and Efron *et al* (1989) were the first to study normal OST thermograms, taking into account differences among ocular regions, but their studies had some limitations. Morgan *et al* (1993) reported *r* values between OST and other

Table 2. General linear models[a] testing the relationship between OST measured from the five ocular regions considered and skin temperature, age and lab temperature. The initial fully adjusted model was reduced to a 'most parsimonious' model by using backward selection.

Nasal area	Coef.	Std. err.	t	$P > \|t\|$	Beta
Skin temperature [°C]	0.76	0.07	10.93	0.000	0.57
Age [Years]	−0.01	0.00	−4.49	0.000	−0.23
Constant	8.48	2.54	3.33	0.001	·
Number of obs	220	R-squared	0.44		
F(2, 217)	86.72	Adj R-squared	0.44		
Prob > F	0.000	Root MSE	0.40		
Nasal-central area	Coef.	Std. err.	t	$P > t$	Beta
Skin temperature [°C]	0.78	0.07	11.68	0.000	0.59
Age [Years]	−0.01	0.00	−4.55	0.000	−0.23
Constant	7.41	2.44	3.04	0.003	·
Number of obs	220	R-squared	0.47		
F(2, 217)	97.1	Adj R-squared	0.47		
Prob > F	0.000	Root MSE	0.38		
Central area	Coef.	Std. err.	t	$P > t$	Beta
Skin temperature [°C]	0.73	0.06	11.43	0.000	0.58
Lab temperature [°C]	0.03	0.01	2.86	0.005	0.14
Age [years]	−0.01	0.00	−4.24	0.000	−0.21
Constant	7.86	2.27	3.46	0.001	·
Number of obs	220	R-squared	0.52		
F(3, 216)	76.93	Adj R-squared	0.51		
Prob > F	0.000	Root MSE	0.35		
Central temporal area	Coef.	Std. err.	t	$P > t$	Beta
Skin temperature [°C]	0.66	0.06	10.29	0.000	0.51
Lab temperature [°C]	0.06	0.01	5.12	0.000	0.25
Age [years]	−0.01	0.00	−5.3	0.000	−0.25
Constant	9.80	2.27	4.31	0.000	·
Number of obs	220	R-squared	0.54		
F(3, 216)	84.07	Adj R-squared	0.53		
Prob > F	0.000	Root MSE	0.35		
Temporal area	Coef.	Std. err.	t	$P > t$	Beta
Skin temperature [°C]	0.61	0.06	9.86	0.000	0.49
Lab temperature [°C]	0.07	0.01	6.15	0.000	0.29
Age [Years]	−0.01	0.00	−5.50	0.000	−0.26
Constant	11.79	2.18	5.41	0.000	·
Number of obs	220	R-squared	0.55		
F (3, 216)	87.85	Adj R-squared	0.54		
Prob > F	0.000	Root MSE	0.34		

[a] The initial fully adjusted model also included lab humidity, gender, cardiovascular risk factors including sedentary subjects, and smoke.

variables (age, oral temperature, etc) without the regression's equations, and did not detail the characteristics of the studied population; Efron *et al* (1989) instead analysed a very small population made of 21 subjects. When investigating the relationship between age and OST, Morgan *et al* (1999) focused on the central corneal surface temperature, so the linear regression analysis and correlation coefficient determination were carried out considering only that area. Years later, Tan *et al* 2009 established an inter-subject OST norm in Chinese young adults (mean age 19), but their results should be confirmed taking into account a population ranging in a wider age span.

The regression model proposed in this study paves the way for further investigation, especially when the normal OST has to be a reference for discriminating pathological conditions that occur in altered OST.

The use of skin forehead temperature as an indicator of body temperature might be a limitation of our study: we suggest using oral temperature for further studies. Furthermore, other aspects could be considered in future

investigations: the reliability of our regression model in other examination room temperature ranges (lower or above 25 °C); OSTs belonging to the left side; and the contribution to the regression model of the BMI instead of body mass and height considered separately.

As OST evaluation can be important in detecting early ocular inflammation, dry eyes, ocular blood flow alterations, glaucoma, maculopathy, uveal lesions, etc, having precise details of the variation in temperature across the ocular surface, and therefore a more detailed map of the OST adjusted according to subject characteristics and environment conditions, could enhance early diagnosis and thus the course of treatments.

5. Conclusion

Infrared thermography is a non-invasive, valid and reliable tool that can be used to acquire OST.

In this study we have investigated normal subjects' OSTs, in order to detect which factors should not be neglected when OST is measured for evaluating ocular conditions and/or finding out the presence of pathological ocular conditions.

Our results suggest that there are three main parameters to be considered: (i) the region dependency of the OST: there is a significant difference in OST among the ocular regions, e.g. the central cornea temperature should not be considered as a reference for the whole OST; (ii) the subjects' factors dependency: age and forehead skin temperature; (iii) the environmental factor dependency: laboratory temperature, even though OST measurements are performed in a controlled room.

Finally, our results can be used as reference values when investigating ocular pathologies that can influence the OST.

Acknowledgments

The authors would like to thank all volunteers who participated to the measurement acquisitions.

ORCID iDs

Sara Matteoli https://orcid.org/0000-0002-6206-0477
Federica Vannetti https://orcid.org/0000-0001-9403-7944

References

Acharya U R, Ng E Y, Yee G C, Hua T J and Kagathi M 2009 Analysis of normal human eye with different age groups using infrared images *J. Med. Syst.* **33** 207–13
Acharya U R, Tan J H, Koh J E W, Sudarshan V K, Yeo S, Too C L, Chua C K, Ng E Y K and Tong L 2015 Automated diagnosis of dry eye using infrared thermography images *Infrared Phys. Technol.* **71** 263–71
Acharya U R, Tan J H, Vidya S, Yeo S, Too C L, Lim W J E, Chua C K and Tong L 2014 Diagnosis of response and non-response to dry eye treatment using infrared thermography images *Infrared Phys. Technol.* **67** 497–503
Betney S, Morgan P B, Doyle S J and Efron N 1997 Corneal temperature changes during photorefractive keratectomy *Cornea* **16** 158–61
Cardona G, Morgan P B, Efron N and Tullo A B 1996 Ocular and skin temperature in ophthalmic postherpetic neuralgia *Pain Clin.* **9** 145–50
Chang T C, Hsiao Y L and Liao S L 2008 Application of digital infrared thermal imaging in determining inflammatory state and follow-up effect of methylprednisolone pulse therapy in patients with Graves' ophthalmopathy *Graefes Arch. Clin. Exp. Ophthalmol.* **246** 45
Chiang H K, Chen C Y, Cheng H Y, Chen K H and Chang D O 2006 Development of infrared thermal imager for dry eye diagnosis *Proc. SPIE* **6294** 629406
Corvi A, Innocenti B and Mencucci R 2006 Thermography used for analysis and comparison of different cataract surgery procedures based on phacoemulsification *Physiol. Meas.* **27** 371–84
Craig J P, Singh I, Tomlinson A, Morgan P B and Efron N 2000 The role of tear physiology in ocular surface temperature *Eye* **14** 635–41
Efron N, Young G and Brennan N A 1989 Ocular surface temperature *Curr. Eye Res.* **8** 901–6
Fatt I and Forester J F 1972 Errors in eye tissue temperature measurements when using a metallic probe *Exp. Eye Res.* **14** 270–6
Faust O, Acharya U R, Ng E Y K, Tan J H and Yu W 2014 Application of infrared thermography in computer aided diagnosis *Infrared Phys. Technol.* **66** 160–75
Fujishima H, Toda I, Yamada M, Sato N and Tsubota K 1996 Corneal temperature in patients with dry eye evaluated by infrared radiation thermometry *Br. J. Ophthalmol.* **80** 29–32
Galassi F, Giambene B, Corvi A and Falaschi G 2007 Evaluation of ocular surface temperature and retrobulbar haemodynamics by infrared thermography and colour Doppler imaging in patients with glaucoma *Br. J. Ophthalmol.* **91** 878–81
Galassi F, Giambene B, Corvi A, Falaschi G and Menchini U 2008 Retrobulbar hemodynamics and corneal surface temperature in glaucoma surgery *Int. Ophthalmol.* **28** 399–405
Hardy J 1934 The radiation of heat from the human body *J. Clin. Invest.* **13** 593–604
Holmberg A 1952 The temperature of the eye during the application of hot packs, and after milk injections *Acta Ophthalmol.* **30** 348–64
Kamao T, Yamaguchi M, Kawasaki S, Mizoue S, Shiraishi A and Ohashi Y 2011 Screening for dry eye with newly developed ocular surface thermographer *Am. J. Ophthalmol.* **151** 782–91
Mapstone R 1968 Measurement of corneal temperature *Exp. Eye Res.* **7** 237–43

Martin D and Fatt I 1986 The presence of a contact lens induces a very small increase in the anterior corneal surface temperature *Acta Ophthalmol.* **64** 512–8
Matteoli S, Coppini D and Corvi A 2018 A novel image processing procedure for thermographic image *Med. Biol. Eng. Comput.* **56** 1747–56
Matteoli S, Favuzza E, Mazzantini L, Aragona P, Cappelli S, Corvi A and Mencucci R 2017 Ocular surface temperature in patients with evaporative and aqueous-deficient dry eyes: a thermographic approach *Physiol. Meas.* **38** 1503–12
Matteoli S, Finocchio L, Biagini I, Giacomelli G, Sodi A, Corvi A, Virgili G and Rizzo S 2016 A thermographic study on eyes affected by age-related macular degeneration: comparison among various forms of the pathology and analysis of risk factors *Infrared Phys. Tech.* **76** 402–7
Mencucci R, Mazzotta C, Corvi A, Terracciano L, Rechichi M and Matteoli S 2015 *In vivo* thermographic analysis of the corneal surface in keratoconic patients undergoing riboflavin-UV-A accelerated cross-linking *Cornea* **34** 323–7
Morgan P B 1994 Ocular thermography in health and disease *PhD Thesis* University of Manchester
Morgan P B, Soh M P and Efron N 1999 Corneal surface temperature decreases with age *Cont. Lens Anterior Eye* **22** 11–3
Morgan P B, Soh M P, Efron N and Tullo A B 1993 Potential applications of ocular thermography *Optom. Vis. Sci.* **70** 568–76
Morgan P B, Tullo A B and Efron N 1995 Infrared thermography of the tear film in dry eye *Eye* **9** 615–8
Mori A, Oguchi Y, Okusawa Y, Ono M, Fujishima H and Tsubota K 1997 Use of high-speed, high-resolution thermography to evaluate the tear film layer *Am. J. Ophthalmol.* **124** 729–35
Murphy P J, Morgan P B, Patel S and Marshall J 1999 Corneal surface temperature change as the mode of stimulation of the non-contact corneal aesthesiometer *Cornea* **18** 333–42
Purslow C and Wolffsohn J 2007 The relation between physical properties of the anterior eye and ocular surface temperature *Optom. Vis. Sci.* **84** 197–201
Purslow C and Wolffsohn J S 2005 Ocular surface temperature: a review *Eye Contact Lens.* **31** 117–23
Purslow C, Wolffsohn J S and Santodomingo-Rubido J 2005 The effect of contact lens wear on dynamic ocular surface temperature *Cont. Lens Anterior Eye* **28** 29–36
Ring E F J and Ammer K 2000 The technique of infrared imaging in medicine *Thermol. Int.* **10** 7–14
Ring E F J and Ammer K 2012 Infrared thermal imaging in medicine *Physiol. Meas.* **33** R33
Sodi A, Giambene B, Falaschi G, Caputo R, Innocenti B, Corvi A and Menchini U 2007 Ocular surface temperature in central retinal vein occlusion: preliminary data *Eur. J. Ophthalmol.* **17** 755–9
Sodi A, Giambene B, Miranda P, Falaschi G, Corvi A and Menchini U 2009 Ocular surface temperature in diabetic retinopathy: a pilot study by infrared thermography. *Eur. J. Ophthalmol.* **19** 1004–8
Sodi A, Matteoli S, Giacomelli G, Finocchio L, Corvi A and Menchini U 2014 Ocular surface temperature in age-related macular degeneration *J. Ophthalmol.* **2014** 281010
Su T Y, Hwa C K, Liu P H, Wu M H, Chang D O, Su P F, Chang S W and Chiang H K 2011 Noncontact detection of dry eye using a custom designed infrared thermal image system *J. Biomed. Opt.* **16** 046009
Tan J H, Ng E Y K and Acharya U R 2010a Evaluation of tear evaporation from ocular surface by functional infrared thermography *Med. Phys.* **37** 6022–34
Tan J H, Ng E Y K, Acharya U R and Chee C 2009 Infrared thermography on ocular surface temperature: a review *Infrared Phys Technol.* **52** 97–108
Tan J H, Ng E Y K, Rajendra Acharya U and Chee C 2010b Study of normal ocular thermogram using textural parameters *Infrared Phys. Technol.* **53** 120–6
Tan L L, Sanjay S and Morgan P B 2016 Static and dynamic measurement of ocular surface temperature in dry eyes *J. Ophthalmol.* **2016** 7285132
Tan L, Cai Z Q and Lai N S 2009 Accuracy and sensitivity of the dynamic ocular thermography and inter-subjects ocular surface temperature (OST) in Chinese young adults *Cont. Lens Anterior Eye* **32** 78–83
Vannetti F, Matteoli S, Finocchio L, Lacarbonara F, Sodi A, Menchini U and Corvi A 2014 Relationship between ocular surface temperature and peripheral vasoconstriction in healthy subjects: a thermographic study *Proc. Inst. Mech. Eng.* H **228** 297–302